

Evolution of force distribution in three-dimensional granular media

S. Joseph Antony

Department of Chemical and Process Engineering, University of Surrey, Guildford GU2 5XH, England

(Received 1 December 1999; revised manuscript received 14 June 2000; published 18 December 2000)

Based on the discrete element method, the nature of normal contact force distribution and the effect of microstructure (contact fabric) on stresses in granular media sheared under constant mean stress condition is analyzed. The particles are tested in a periodic cell, having a nearly monodispersed system of spherical particles (“hard” and “soft”). The granular systems were initially isotropically compressed to have different solid fractions in order to obtain “dense” and “loose” samples. To study the nature of the force distribution, the granular medium was considered as both (i) noncohesive and (ii) with low values of interface energy. For the granular systems considered here, the nature of force distribution is shown to be dependent on shear history. The amount of interface energy introduced in the granular system does not seem to change the nature of normal force distribution significantly. However, it improves the postpeak stability in agreement with previous research [C. Thornton, *Geotechnique* **50**, 43 (2000)]. The simulation of systems subjected to quasi-static shearing, in general, reveals that in a hard system (both dense and loose), the normal contact force distribution (i) at “peak” shear strength is purely an exponential decay throughout the entire range of force scale that is used, and (ii) at “isotropic” and “steady” states, the contact normal force distribution is bimodal with forces greater than average decaying exponentially at both the states, while the forces less than average tend to be half-Gaussian at the “isotropic” state and a second-order polynomial function at the “steady” state. For the soft (dense) system, the normal contact force distribution at “peak” shear strength is bimodal with forces greater than average decaying exponentially while the forces less than average tend to be a second-order polynomial function. However, for the soft system at both “isotropic” and “steady” states, the contact normal force distribution is half-Gaussian throughout the entire range of force scale that is used. It has been pointed out that in a granular system undergoing slow shearing, the shear strength of the system seems to depend on the ability of the material to form strong fabric anisotropy of contacts carrying strong (greater than average) force.

DOI: 10.1103/PhysRevE.63.011302

PACS number(s): 45.70.-n, 87.18.Bb, 87.64.Aa, 05.45.-a

I. INTRODUCTION

Granular materials are composed of a large number of solid particles that interact with each other at contact points when loaded at the boundary. The study of force and stress fluctuations in a bulk of granular media is a subject of current interest [1–13]. Attempts have been made to search for a better understanding of the contact force distribution in granular materials and to find its correlation to the macroscopic stress [4,8,13] or the bulk dynamic property, for example in the low-velocity regime [1].

In granular media, the transmission of forces from one boundary to another can occur only via the interparticle contacts. Hence the distribution of contacts will determine the distribution of forces within the system of particles. These forces will not necessarily be distributed uniformly. This important qualitative observation of stress distribution can be seen in photoelastic studies of two-dimensional disks reported by many investigators [14–17]. The inhomogeneous distribution of optical fringe patterns in these studies, even for a homogeneous applied load, reveals that the load is transmitted by relatively rigid, heavily stressed chains of particles that form a relatively sparse network of larger than average contact forces. The groups of particles separating the strong force chains are only lightly loaded. There has been a surge of activities at present to identify the probability distribution of contact normal forces in granular media. The knowledge of this distribution would lead to a suitable physical model. For example, the q model [9,16,18], based on a

mean-field solution, has predicted an exponential decay over the whole range of forces. This significant result has led to the possibility of finding a relatively higher probability for normal forces greater than average. Behringer and Miller [19] have conducted experiments to study the effect of fluctuations in the normal stress in a relatively slow granular shear flow. Their predictions compare well with the results obtained using the q model. The improved q model, called the α model, proposed recently by Socolar [20], has predicted that for a two-dimensional system of noncohesive particles in a periodic cell, the force distribution is similar to the one obtained in the q model. However, the “toy” model proposed recently by Sexton *et al.* [10] has predicted the probability distribution of forces as Gaussian at all stages of compression and shows no evidence of an exponential tail. Using molecular-dynamics and contact-dynamics simulations, Radjai *et al.* [21–23] have shown that in a two-dimensional system, the normal contact forces less than average follow a power-law distribution, while the normal contact forces greater than average follow an exponential decay. The recent discrete element simulation by Thornton and Antony [11] on a three-dimensional system of particles has predicted a similar behavior of power-law variation for forces less than half the value of average and an exponential decay for forces greater than average. Although a single model does not fit to their data for the entire range of forces, a model with the same form as that of the q model fits the force distribution greater than the average well. However, a purely empirical model proposed by Mueth *et al.* [7] pro-

vides an excellent fit to their data as well as for the simulation on a three-dimensional packing performed by Radjai *et al.* [8]. The experiments conducted by Mueth *et al.* [7] have predicted a nearly uniform probability distribution for contact normal forces less than the average value.

Although a consensus on the nature of the distribution of contact forces in granular media and a “perfect” physical model to capture the force distribution is far from having been achieved, recent numerical simulations on a two-dimensional [21–24] and three-dimensional system of particles [8,11,24] under quasistatic shearing have revealed some exciting features. It has been shown that the normal force contribution is the major contribution to the total stress tensor and the spatial distribution of normal contact forces can be divided into two subnetworks, viz., (i) the contacts carrying less than the average force (forming “weak force chains”) and (ii) the contacts carrying greater than the average force (forming “strong force chains”). The contacts that slide are predominantly in the weak force chains and they contribute only to the mean stress while their contribution to the deviator stress (shear strength) is negligible. The contribution of the strong force chains to the deviator stress is the dominant contribution. Hence, the weak force chains play a role similar to a fluid surrounding the solid backbone composed of the strong force chains. A recent investigation [25] for hydrodynamic interactions on concentrated system also reveals that the distribution of stresses in flowing aggregated suspensions exhibits similarities with the stress distribution in granular systems, characterized by approximately exponential decay at large stresses.

The present paper gives results based on discrete element method simulations for the evolution of the contact normal force distribution in a nearly monodispersed system of particles. The particles were tested in a periodic cell having a large solid spherical particle submerged in a bed of monodispersed spherical particles. The single large solid spherical particle (whose diameter is five times greater than that of the surrounding particles) is referred as a “submerged particle.” It is of interest to analyze how the system of particles responds to the force transmission and the associated features during slow shearing. The specific objectives of the present investigation are to study the evolution of normal contact force distribution in granular system with (i) noncohesive particles (interface energy $\Gamma = 0 \text{ J/m}^2$) and (ii) low values of interface energy ($\Gamma = 0.6, 6, 12, \text{ and } 20 \text{ J/m}^2$). The effect of the solid fraction (relatively “dense” and “loose”) and modulus of elasticity of particles (relatively “hard” and “soft”) on the normal force distribution has been considered. It will be shown that for granular systems sheared under the high constant mean stress condition, the nature of normal force distribution for particles with low interface energies (considered in this study) is characteristically not very different from that of noncohesive particles. Particular attention has been paid to study the shear resistance characteristics of these granular systems during slow shearing. It has been pointed out that the shear resistance of quasistatic granular systems seems to depend on the ability of the material to form a strong anisotropic fabric network of contacts carrying strong (greater than average) force.

II. SIMULATIONS

The simulations are carried out using the discrete element method (DEM), which was originally developed by Cundall and Strack [26]. The method models the interaction between contiguous particles as a dynamic process and the time evolution of the particles is advanced using an explicit finite difference scheme. The interaction between the neighboring particles is modeled by algorithms based on theoretical contact mechanics provided by Thornton and Yin [27] and Thornton [28]. For the detailed information about the numerical methodology, the reader should refer to Cundall and Strack [26]. The advantage of using the DEM with granular materials is its ability to give more information about what happens inside the system. This enhances the understanding of the physics of the granular media.

The simulations are carried out in a three-dimensional cuboidal periodic cell having a nearly monodispersed system of particles. A large spherical particle with a diameter 0.05 mm was generated at the center of the periodic cell and was surrounded by 5000 monosized spherical particles with a diameter 0.01 mm, initially randomly located within the accessible domain of the cell. These particles were generated in one million trials. At this stage, the particles were having no contacts. It is worth noting that the two ways to achieve a large number of particles generated in a periodic cell are by increasing either the size of the periodic cell or the number of trials. The former may be difficult and also time-consuming during the isotropic compression stages, while the latter may take a considerably long time. Keeping the right balance between these two methods could be sufficient to generate the granular assembly of interest. All the particles were given the following properties: Young’s modulus, $E = 70 \text{ GPa}$ (“hard”) or 70 MPa (“soft”), Poisson’s ratio $\nu = 0.3$, coefficient of interparticle friction $\mu = 0.3$, and different values of interface energy, viz., $\Gamma = 0.6, 6, 12, \text{ and } 20 \text{ J/m}^2$. After the particles were initially generated, the system was isotropically compressed until a mean stress $p = 1 \text{ kPa}$ was obtained using a numerical algorithm of the following form:

$$\dot{\epsilon} = \dot{\epsilon} + g(p_d - p_0). \quad (1)$$

In the above equation, $\dot{\epsilon}$ is the strain rate, p_d is the desired isotropic stress, and p_0 is the obtained isotropic stress at a particular stage. An initial strain rate of 10^{-5} s^{-1} was specified that was progressively modified according to Eq. (1) using a value for the gain parameter (g) calculated from

$$g = [\dot{\epsilon}/(p_d - p_0)]_{\text{initial}}. \quad (2)$$

Equations (1) and (2) ensure that the strain rate decreases as the stress difference decreases and that the strain rate tends to zero as the calculated value of the isotropic stress approaches the desired value, thereby bringing the system to equilibrium. In order to get a stable system at the desired stress level, calculation cycles were continued until the solid fraction and coordination number had attained constant values. This procedure was used to progressively raise the isotropic stress to create different samples having an isotropic stress

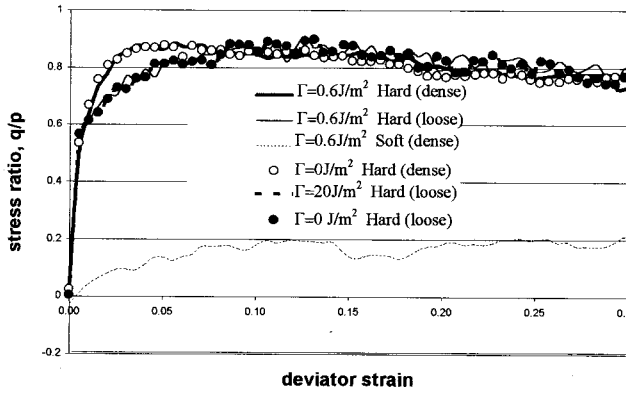


FIG. 1. Variation of stress ratio, q/p , during shearing [$q = \sigma_1 - \sigma_3$, $p = (\sigma_1 + \sigma_2 + \sigma_3)/3$].

level of either 20 or 100 kPa. The sample with an isotropic stress of 100 kPa is referred to as the “dense” sample and the sample with an isotropic stress of 20 kPa is referred to as the “loose” sample. In total, three samples were prepared, viz., two “hard” samples (dense and loose with solid fractions 0.633 and 0.618, respectively) and a soft sample (dense, with a solid fraction 0.69). At the end of isotropic compression, the microstructure of the samples was isotropic. The mechanical coordination numbers at the isotropic state for the two hard systems (dense and loose) and the soft system were 5.689, 4.76, and 7.70, respectively. For shearing, a strain rate of 10^{-5} s^{-1} was employed in the simulations. The samples were subjected to the axisymmetric compression test ($\sigma_1 > \sigma_2 = \sigma_3$). During shearing, the mean stress $p = (\sigma_1 + \sigma_2 + \sigma_3)/3$ was maintained constant at 100 and 20 kPa for the dense and loose samples, respectively, using the numerical algorithm.

III. RESULTS AND DISCUSSION

Figure 1 shows the normalized shear strength (stress ratio q/p) for the granular systems during shearing (deviator strain $\varepsilon_1 - \varepsilon_3$). The stress ratio is defined as the ratio of deviator stress $q = (\sigma_1 - \sigma_3)$ to the mean stress p . In this figure, the results for the case of particles with surface energy $\Gamma = 0.6 \text{ J/m}^2$ are presented for hard (dense and loose) systems. The results corresponding to the noncohesive ($\Gamma = 0 \text{ J/m}^2$) hard (dense) system are incorporated for comparison. From this figure, it can be observed that the variation of the stress ratio for the noncohesive hard (dense) system is not significantly different from that of particles with $\Gamma = 0.6 \text{ J/m}^2$. Also, no significant further deviation was observed for the hard (dense) system of particles tested with $\Gamma = 6, 12,$ and 20 J/m^2 and hence it is not presented here. However, comparing the q/p curves for the cases of hard (dense) systems with $\Gamma = 0$ and 0.6 J/m^2 indicates that the presence of interface energy of particles could improve the stability of the system (especially postpeak behavior) sheared under the high constant mean stress condition, as reported in another recent study [12]. In Fig. 1, for the hard (loose) system, the typical results corresponding to $\Gamma = 0$ and 20 J/m^2 are also incorporated for comparison. Again, no signifi-

cant deviation of the q/p curve was observed with that of $\Gamma = 0.6 \text{ J/m}^2$, except that the increase in interface energy seems to improve the stability of the q/p curve. For the hard (loose) system, the results corresponding to $\Gamma = 6$ and 12 J/m^2 are not presented here, as there was no significant deviation observed with that of $\Gamma = 0$ and 0.6 J/m^2 . To summarize, it can be said that for granular systems sheared under the (high) constant mean stress condition, an increase in the value of interface energy of particles does not seem to significantly affect the overall behavior of the q/p curve with that of the noncohesive granular system, nevertheless it could improve stability, especially during postpeak behavior. Hence for the further analysis carried out in this paper, the samples with interface energy $\Gamma = 0.6 \text{ J/m}^2$ are considered, unless stated otherwise. In the following, we probe further some features of the q/p curve and the evolution of the force distribution. To evaluate the behavior of the q/p curve in detail, the results corresponding to a soft (dense) system (with interface energy $\Gamma = 0.6 \text{ J/m}^2$) are also incorporated in Fig. 1 for comparison.

Although the normalized stress ratio q/p (Fig. 1) for both cases of the hard system (dense and loose) attained fairly the same value at peak ~ 0.88 , the dense system attained a peak far earlier than that of the loose system during shearing. The dense system attained “peak” shear strength at deviator strain 0.035, and the loose system attained peak shear strength at deviator strain 0.111. Both the dense and loose systems attained the “steady” state at deviator strain ~ 0.15 . In the case of the soft system, the stress ratio q/p curve increases at a lower rate than that of the hard system. For the soft system, a well-defined peak in the q/p curve is not observed, unlike in the hard system. However, after a considerable drop in the value of q/p at deviator strain 0.15, the soft system attained the maximum value of q/p (~ 0.2) at about a deviator strain 0.197. For the soft system, this state is referred to as “peak” here. At this point in time, we are not very aware of the reasons that control the behavior of the shear strength curve (q/p). However, later in this paper, an attempt will be made to look into this aspect, and a possible link with the nature of force distribution in the granular systems during shearing is discussed. Let us now look into the nature of force distribution in the granular systems (selected here) subjected to slow shearing.

Recent numerical simulations (for example, [11]) have shown that the normal contact force contribution is the dominant contribution to the deviator stress tensor, whereas the tangential contact force contribution is very small during slow shearing. This behavior has also been observed in the present simulations. Hence it is of interest to look in detail at the evolution of the probability distribution of the contact normal force in the system.

A. Nature of force distribution

Figure 2 shows the evolution of normal contact force distribution for a typical noncohesive hard (dense) granular system during shearing. Figures 3–5 show the evolution of the probability distribution of the contact normal force for the hard and soft systems with interface energy ($\Gamma = 0.6 \text{ J/m}^2$)

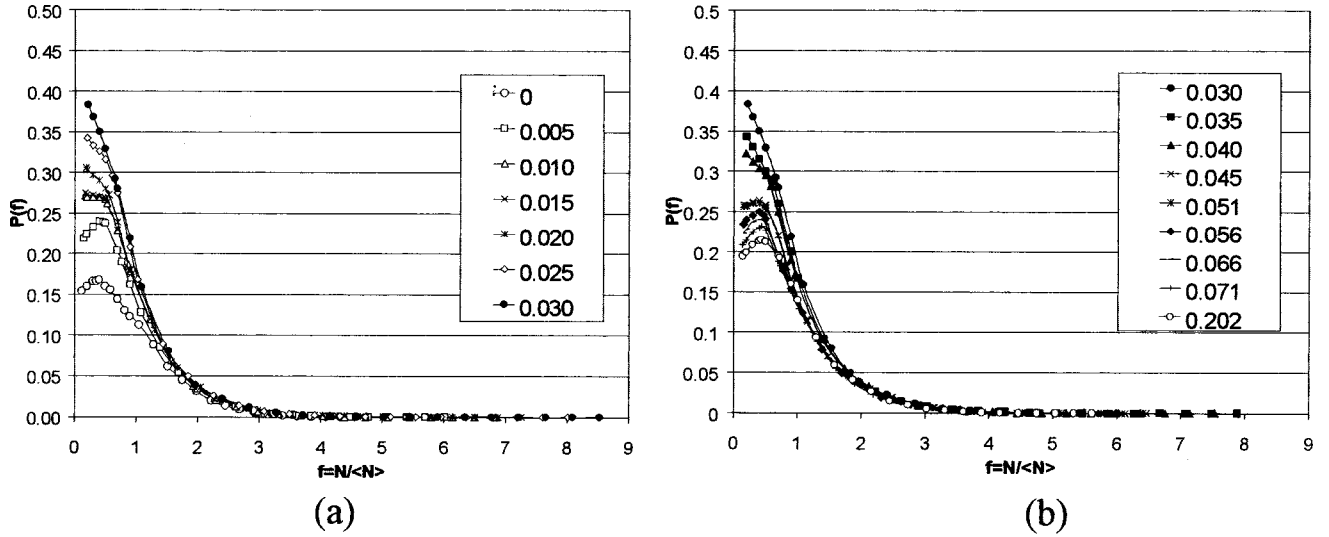


FIG. 2. Evolution of the probability distribution of contact normal forces for the noncohesive hard (dense) granular system during shearing. The numbers in the legend correspond to the deviator strain.

during shearing. From these figures, it is interesting to note that the probability distribution of contact normal force is shear-state-dependent, even for a noncohesive granular system. The evolution of force distribution for the case of the noncohesive hard (loose) system is not presented as it was not characteristically very different from that of the granular system with interface energy $\Gamma=0.6$ J/m² (as one would expect from Fig. 1). Although the intention is not to fit a model for force distribution for all stages of shearing, it is attempted to fit the present data for some selected states, viz., isotropic (before shearing), peak, and steady states; see Figs. 6 and 7.

1. Noncohesive granular system

We analyze the nature of force distribution for a typical case of the noncohesive hard (dense) granular system. It is observed that, for the isotropic state [Fig. 6(a)], the probability distribution for contact normal forces fits reasonably well with the same form as that of the q model with $k=2$ as

$$P(f) = [k^k / (k-1)!] f^{k-1} e^{-kf}, \quad (3)$$

where $f=N/\langle N \rangle$ and $\langle N \rangle$ is the average contact normal force. However, it can be noted that the probability distribution function for contact normal forces less than average fits well with the half-Gaussian distribution defined as

$$P(f) = Y_0 + \frac{A}{w\sqrt{\pi/2}} e^{-2(f-X_c)^2/w^2} \quad (4)$$

with $Y_0=0.103$, $X_c=0.358$, $w=0.716$, and $A=0.057$. For the forces greater than average, the probability distribution of contact normal force is exponential with

$$P(f) \propto e^{-\beta(f-1)} \quad (5)$$

and $\beta=1.440$.

For a further increase in deviator strain, the force distribution gradually changes, and at ‘‘peak’’ state the probability distribution [Fig. 6(b)] for contact normal force decays exponentially with

$$P(f) \propto e^{-\beta f} \quad (6)$$

and $\beta=1.100$, remarkably throughout the entire force scale that is used. As the deviator strain increases further, the force distribution curve gradually swings back (Fig. 2) and attains a bimodal distribution at the steady state. At steady state, a good polynomial fit is obtained for the forces less than average in the following form:

$$P(f) = A + Bf + Cf^2 \quad (7)$$

with $A=0.171$, $B=0.194$, and $C=-0.223$. At steady state, the probability distribution for contact normal force greater than average is exponential as defined in Eq. (5), with $\beta=1.480$.

2. Granular system with interface energy

Now, let us look into the nature of force distribution for the hard (dense and loose) and soft (dense) granular systems with a typical interface energy ($\Gamma=0.6$ J/m²).

For the hard dense system at isotropic state [Fig. 7(a)], the probability distribution function for contact normal forces less than average fits well with the half-Gaussian distribution defined in Eq. (4) with $Y_0=0.046$, $X_c=0.520$, $w=0.845$, and $A=0.126$. For forces greater than average, the probability distribution of contact normal force decays exponentially as defined in Eq. (5) with $\beta=1.410$. For a further increase in deviator strain, the force distribution gradually changes, and at the ‘‘peak’’ state the probability distribution [Fig. 7(b)] for the contact normal force decays exponentially as defined in Eq. (6) with $\beta=1.200$, remarkably throughout the entire force scale that is used. As the deviator strain increases further, the force distribution curve gradually swings back (Fig.

3) and attains a bimodal distribution at the steady state. At steady state, a good polynomial fit is obtained for the forces less than average as defined in Eq. (7) with $A=0.189$, $B=0.202$, and $C=-0.248$. At steady state, the probability distribution for contact normal force greater than average decays exponentially as defined in Eq. (5), with $\beta=1.420$.

For the hard loose system in the isotropic state [Fig. 7(c)], the contact normal force distribution for forces less than average fits well with the half-Gaussian distribution as defined in Eq. (4) with $Y_0=0.024$, $X_c=0.279$, $w=1.487$, and $A=0.318$. For forces greater than average, the contact normal force distribution is exponential as defined in Eq. (5) with $\beta=1.420$. For a further increase in deviator strain, the force distribution gradually changes, and at the ‘‘peak’’ state, as in the hard dense system, the probability distribution for the contact normal forces [Fig. 7(d)] tends to decay exponentially as defined by Eq. (6) with $\beta=2.140$, remarkably throughout the entire force scale that is used. As the system is sheared further, the force distribution swings back and fluctuates in a short range of deviator strain (Fig. 4), before eventually attaining the steady state. At the steady state, a

good polynomial fit is obtained for forces less than average as defined by Eq. (7) with $A=0.214$, $B=-0.035$, and $C=-0.052$. For forces greater than average at steady state, the contact force distribution decays exponentially as defined in Eq. (5) with $\beta=1.350$.

For the soft system, the normal contact force distribution is found to be entirely half-Gaussian at the ‘‘isotropic’’ and ‘‘steady’’ states [Fig. 7(e)], as defined by Eq. (4). The fit parameters used in Eq. (4) for the isotropic state are as follows: $Y_0=0.001$, $X_c=0.548$, $w=1.559$, and $A=0.283$. For the steady state, the fit parameters are as follows: $Y_0=0.001$, $X_c=0.498$, $w=1.666$, and $A=0.276$. However, at the ‘‘peak’’ state, the contact force distribution is bimodal, unlike in the hard system where the contact force distribution at ‘‘peak’’ shear strength tends to be an exponential decay throughout the entire force scale that is used. The contact normal force distribution with forces less than average seems to fit well with a second-order polynomial function as defined by Eq. (7) with $A=0.207$, $B=0.274$, $C=-0.298$, whereas forces greater than average decay exponentially as defined by Eq. (5) with $\beta=1.510$.

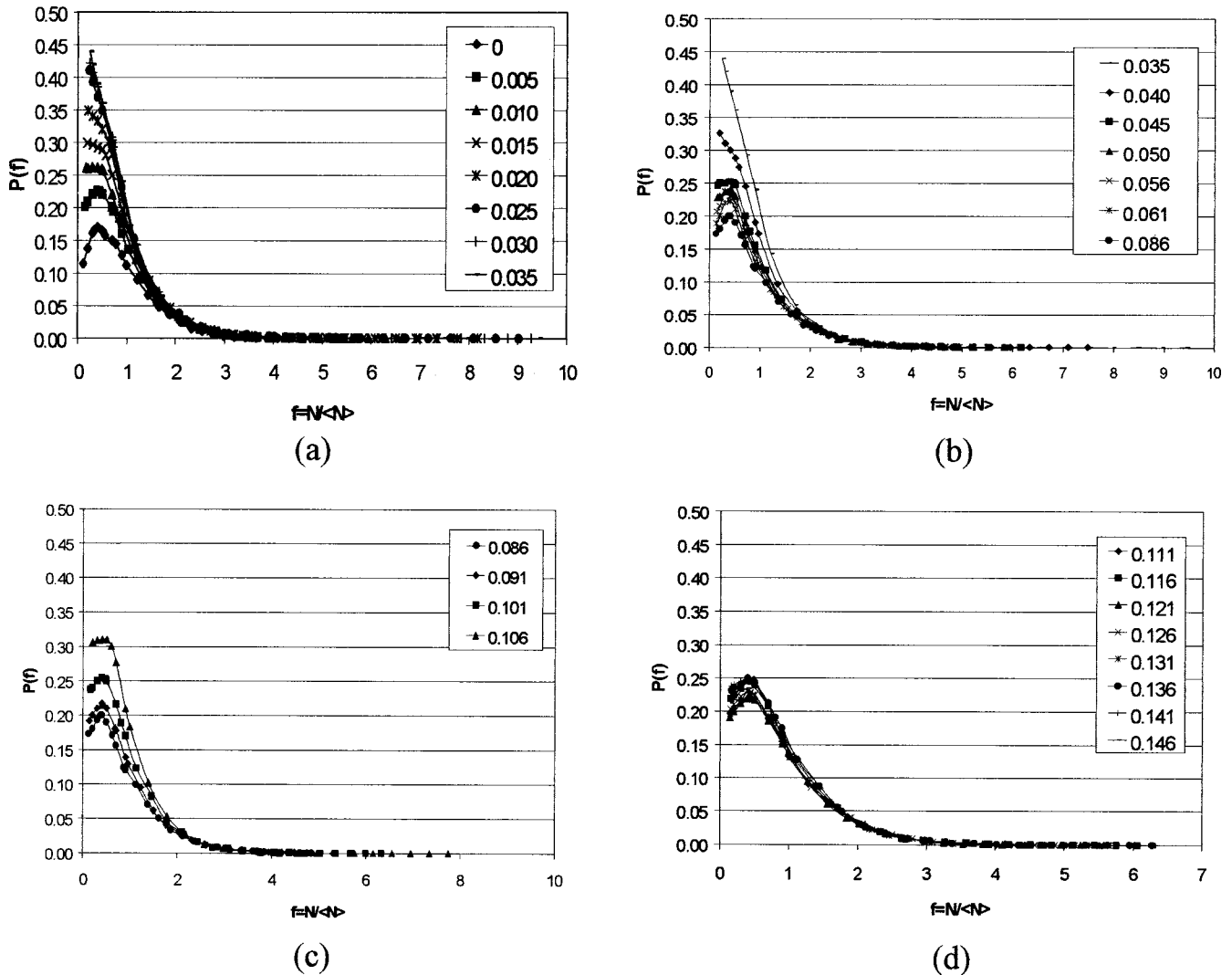


FIG. 3. Evolution of the probability distribution of contact normal forces for the hard (dense) granular system during shearing. The numbers in the legend correspond to the deviator strain.

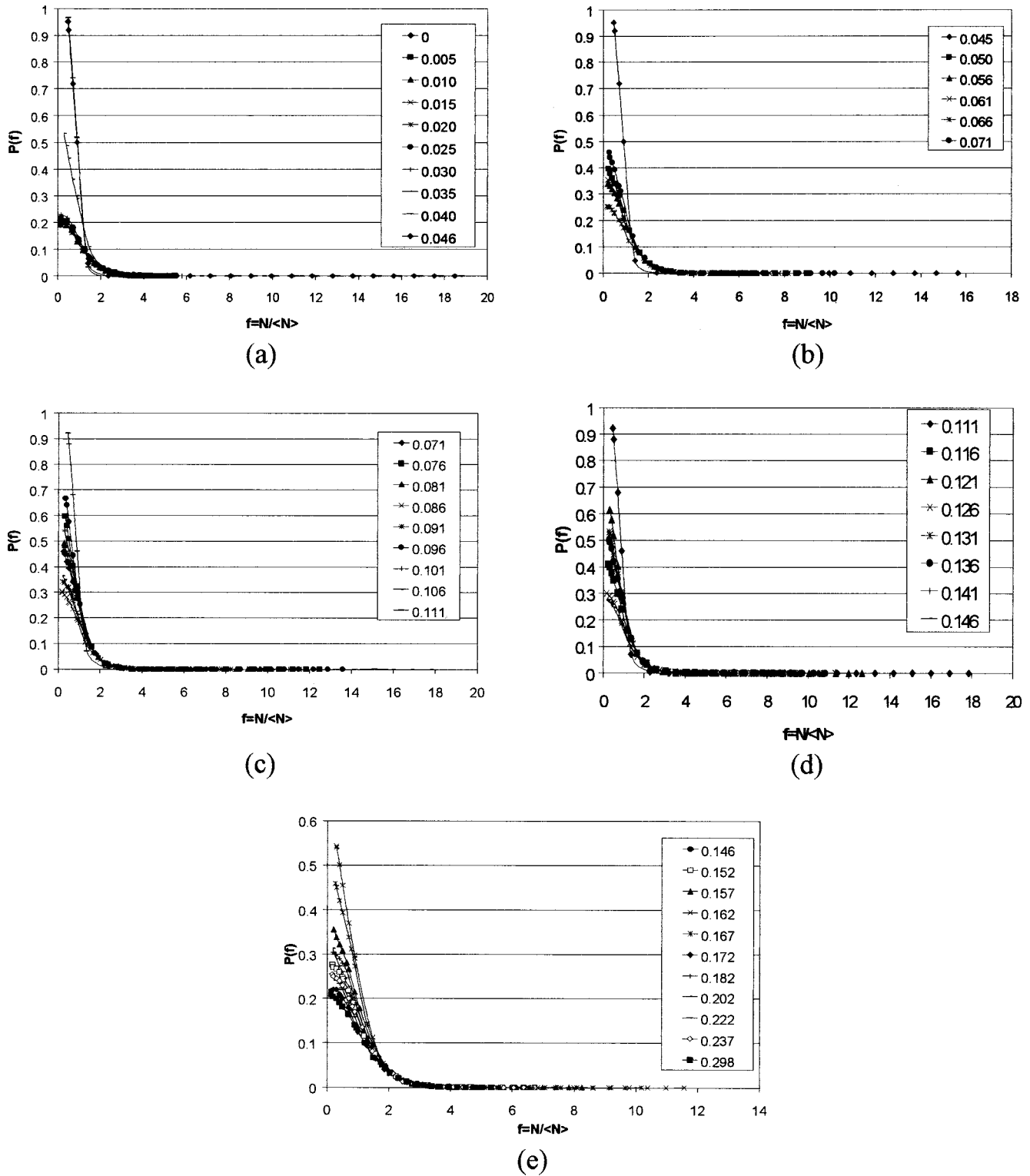


FIG. 4. Evolution of the probability distribution of contact normal force for the hard (loose) granular system during shearing. The numbers in the legend correspond to the deviator strain.

B. Features of the contact force, contact fabric, and their possible correlation to shear strength (q/p) curves

In the previous sections we observed that the nature of force distribution in granular media during slow shearing depends on the shear history. A natural question now arises:

Does the nature of force distribution and the associated contact structure (fabric) influence the q/p curves (Fig. 1) in any way? Although one would intuitively expect that the nature of force distribution and the contact fabric would have a strong role to play in building up the shear strength, this

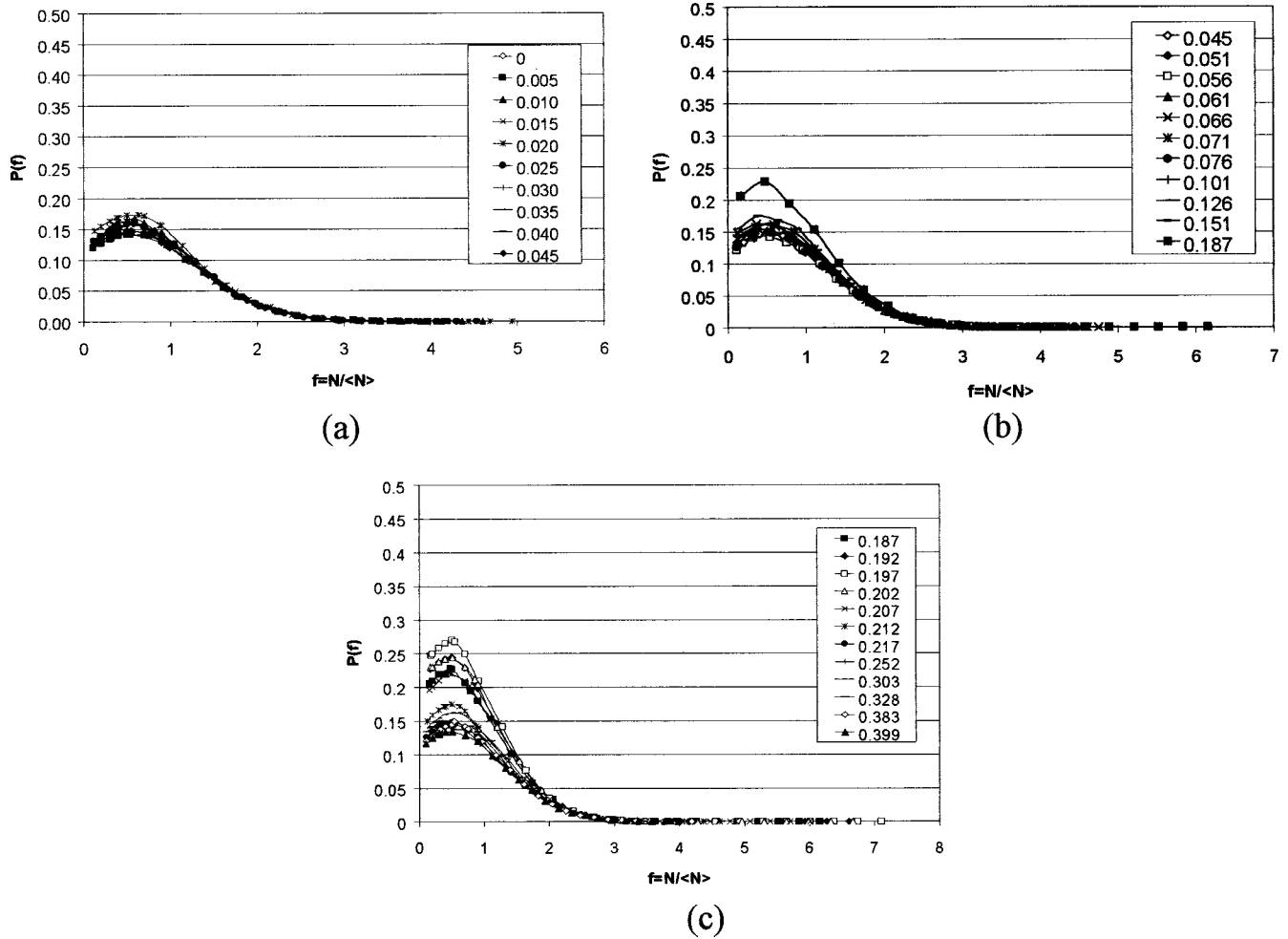


FIG. 5. Evolution of the probability distribution of contact normal forces for the soft (dense) granular system during shearing. The numbers in the legend correspond to the deviator strain.

aspect is not yet well understood. In this section, we probe in detail the contribution of force chains and their structure to the shear strength.

As presented earlier in Fig. 1, one could observe that the normalized stress ratio q/p at “peak” for the soft system is far lower (~ 0.2) than that of the hard system (~ 0.88). Although the soft system presented here is dense, we could not observe a well-defined peak in its q/p variation curve. Recently, Thornton and Antony [29] have carried out a numerical simulation for the slow shearing of a soft (dense, solid fraction 0.685) particulate system. It is interesting to note in their simulation that the elastic properties of the particles had the same values as that of the one considered (soft) in the present study. However, the only difference is that, in their simulation, they considered the particles as polydispersed (in size). They have reported a defined peak in the q/p curve (q/p is ~ 0.75) occurring at deviator strain ~ 0.15 . Although one may expect a higher value of shear strength for a polydispersed system than that of a monodispersed system when other properties of the systems are identical, the shear strength observed for the soft system in the present study is quite low, and this has motivated us to probe further.

As presented in the Introduction, one could recall that the contacts that slide are predominantly in the weak force

chains and they contribute only to the mean stress while the strong force chains contribute to the deviator stress (shear strength). Also, the normal contact force contribution is the dominant contribution to the deviator stress tensor, whereas the tangential contact force contribution is very small during slow shearing. Hence it would be of interest to evaluate the contribution of the contacts having greater than average normal contact force coupled with their structure during shearing.

Figure 8 shows, for the granular systems (with interface energy $\Gamma = 0.6 \text{ J/m}^2$), the evolution of the maximum value of contact normal force experienced by the systems during shearing. This is presented in terms of plotting the maximum value of “ f ” found in the corresponding force distribution graphs (Figs. 3–5), irrespective of the number of times they occur (probability values) at this instance. From this figure, the following observations could be made: (i) for all the systems considered here, the maximum value of the normal contact force observed at states corresponding to the “peak” shear strength is far higher than that of their neighborhood deviator strain levels; (ii) at “steady” state, interestingly for all the systems considered here, the maximum value of the normal contact force seems to have attained nearly the same

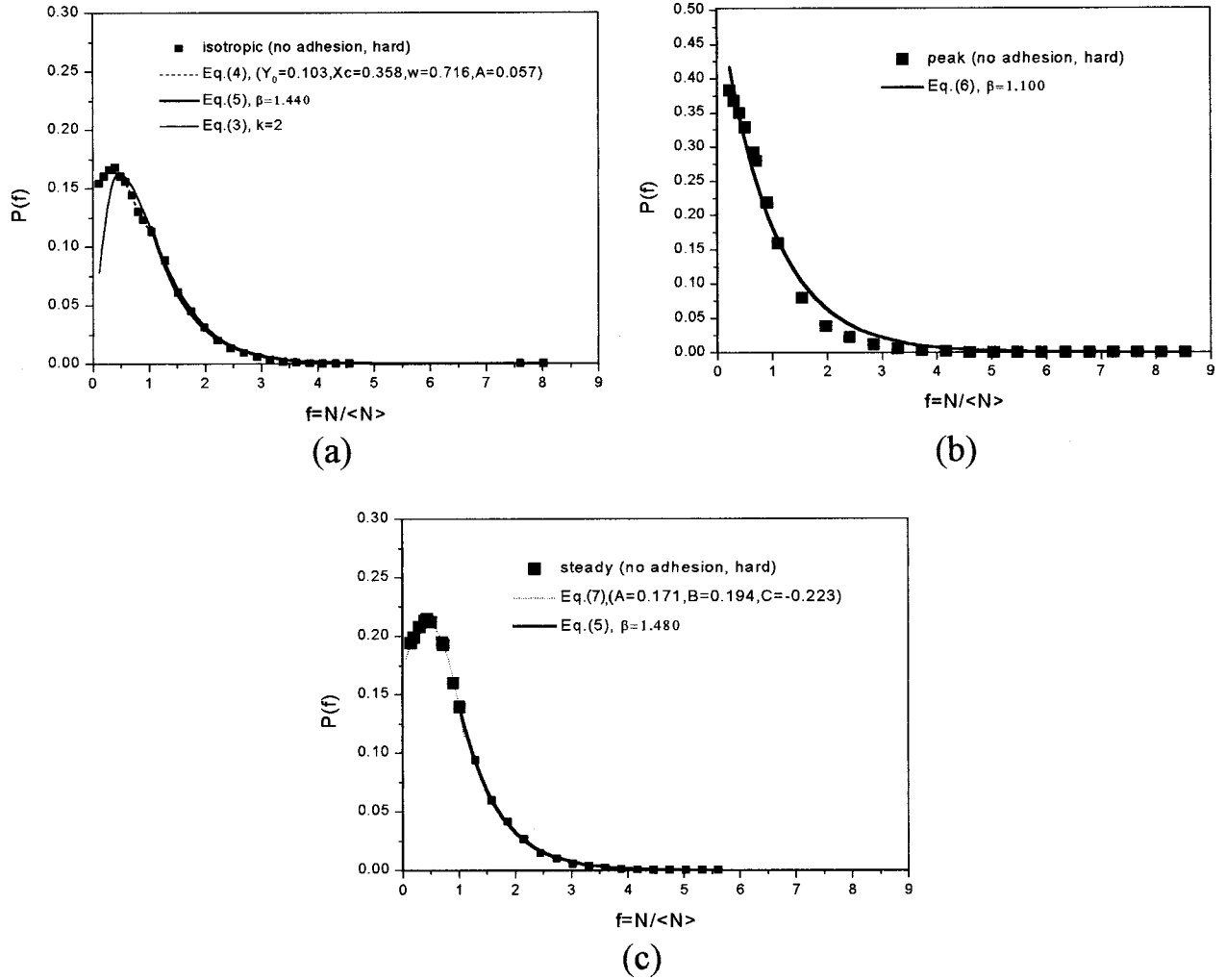


FIG. 6. Best fits for the probability distribution of contact normal force for the noncohesive hard (dense) granular systems during shearing.

value. We are aware that, at steady state (sometimes referred to as “critical state”), the granular system would attain a “critical density.” At the critical state, the system is expected to attain a uniform variation in mechanical coordination number (average number of load-bearing contacts). One may observe from Fig. 9 that, at steady state, the systems have attained a stable, nearly uniform value of the mechanical coordination number. We have now observed that at the “critical state,” the systems seem to have attained a unique value of the maximum normal contact force as well. From Figs. 3–5, 8, and 9, one could further observe that during shearing, the contacts seem to undergo a continuous compression and relaxation of the force chains, though the mechanical coordination number remains fairly uniform for most of the shearing.

Now, let us focus our attention on coupling the group of contacts (in terms of structure) that are carrying the strong forces and their evolution during shearing. To do this, the structural anisotropy in the granular assembly is defined by the distribution of contact orientations, which may be defined by a “fabric tensor” ϕ_{ij} , suggested by Satake [30] as

$$\phi_{ij} = \langle n_i n_j \rangle = \frac{1}{M} \sum_1^M n_i n_j, \quad (8)$$

where M is the number of contacts in the representative volume element and n_i defines the components of the unit normal vector at a contact between two particles.

Figure 10 shows the variation of (a) the deviator fabric ($\phi_1 - \phi_3$) and (b) the deviator fabric of contacts with strong forces ($f > 1$), for the hard and soft systems during shearing. From this figure, it may be observed that the hard system is far more strongly anisotropic than the soft system. The maximum degree of structural anisotropy [Fig. 10(a)] developed for the hard dense and loose systems is ~ 0.125 and ~ 0.15 , respectively, whereas for the soft (dense) system it is ~ 0.022 . At steady state, the maximum degree of structural anisotropy for the hard dense and loose systems is ~ 0.105 and 0.14 , respectively, whereas for the soft system it is ~ 0.02 . It may be pointed out here that, for the polydispersed soft system simulated by Thornton and Antony [29], it has been shown that a maximum structural degree of anisotropy is obtained at a value of ~ 0.065 , reducing to 0.045 for the

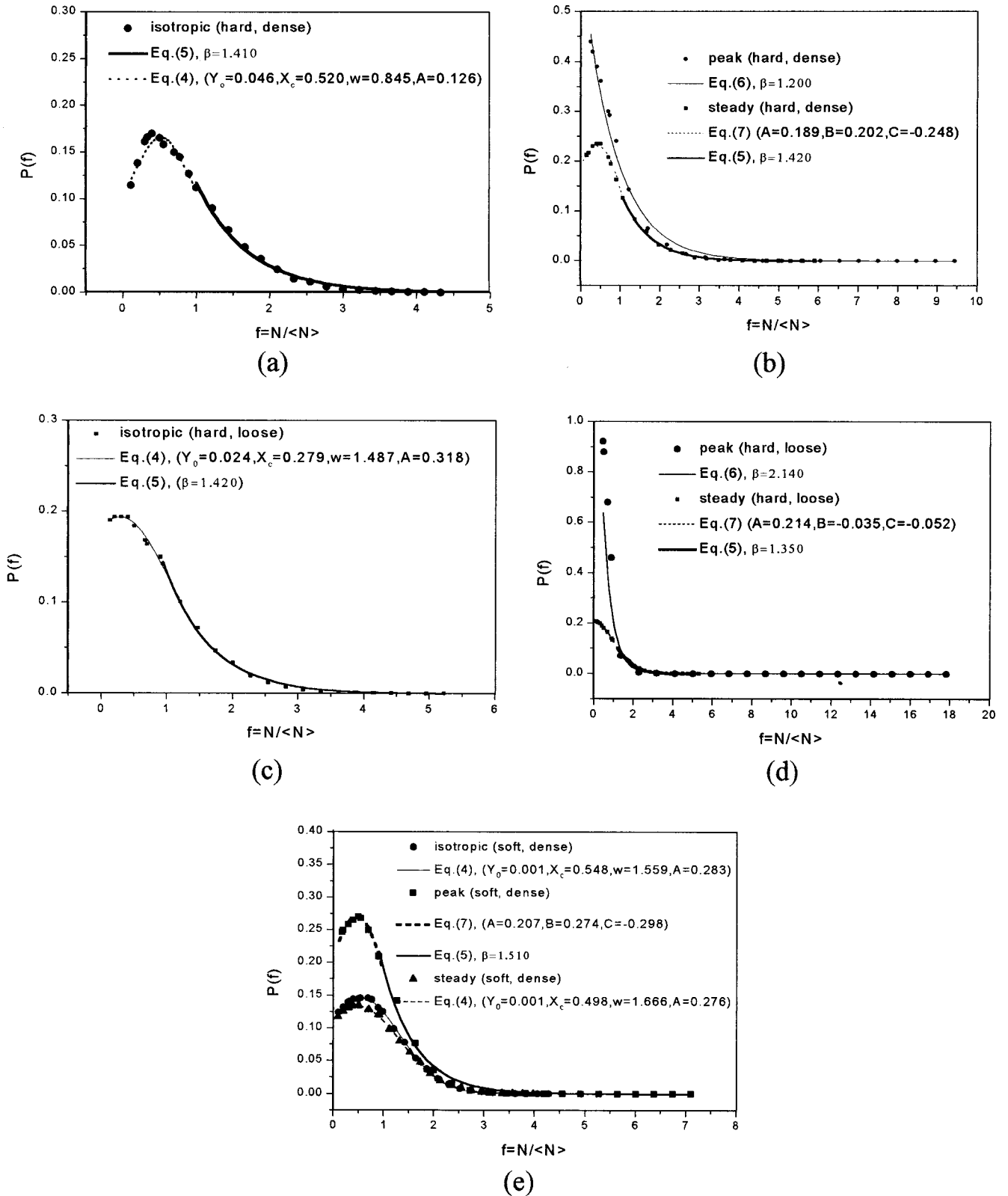


FIG. 7. Best fits for the probability distribution of contact normal force for the hard and soft granular systems during shearing.

steady state. These values clearly demonstrate that the induced structural anisotropy developed during shearing is significantly dependent on the elastic modulus of the particles and the solid fraction of the granular system. Figure 10(b)

shows the evolution of the deviator fabric of strong contacts ($f > 1$) within the overall system. It may be observed that there is a strong anisotropic structure for contacts carrying strong forces within the overall system. One can also observe

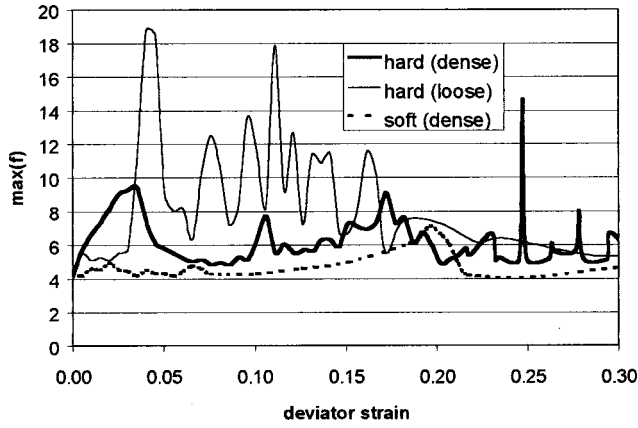


FIG. 8. Variation of the maximum contact normal force during shearing.

that fabric anisotropy of strong contacts for the soft system considered in this study is far less anisotropic than the hard systems. It shall be pointed out here that the polydispersed soft system simulated by Thornton and Antony [29] has shown a maximum structural degree of anisotropy value for the strong contacts as ~ 0.275 , reducing to ~ 0.25 in the steady state. This clearly demonstrates that the developed induced structural anisotropy of the strong contacts in the soft system considered in the present study is relatively weak.

The structural anisotropy tensor ϕ_{ij} may further be decomposed as follows [11]:

$$\phi_{ij} = (1 - \nu) \phi_{ij}^w + \nu \phi_{ij}^s, \quad (9)$$

where the superscripts “w” and “s” indicate the weak and strong force subnetworks and “ ν ” is the proportion of contacts with $f > 1$. As reported earlier, in the present simulations the subnetwork of contacts with $f > 1$ develops a strong anisotropic structure, and the weak subnetworks were nearly isotropic [11,21–24,29], though this is not presented here. In order to examine the contribution of the subnetwork of contacts with strong forces, it is useful to define the fabric stress σ_{ij}^f as [31]

$$\sigma_{ij}^f = \sigma_{kk} \phi_{ij}. \quad (10)$$

Thornton had assumed that [31] the deviator stress (q) is equal to the fabric deviator stress contribution of contacts transmitting greater than average normal contact force. Figure 11 shows the variation between the deviator stress and the fabric deviator stress due to contacts carrying forces greater than average [i.e., $\sigma_{kk}(\phi_1 - \phi_3)^s$]. From this figure it can be observed that, for both the cases of hard systems, the deviator stress variation is nearly equal to the fabric deviator stress due to contacts with $f > 1$. Although there is a linear variation of this in the case of soft systems, the fabric stress contribution of contacts with $f > 1$ is only about half the deviator stress, or in other words, the soft system considered here is unable to build up the strong ($f > 1$) anisotropic structure to mobilize the shear strength. It is worth stating here that, for the soft system examined by Thornton and

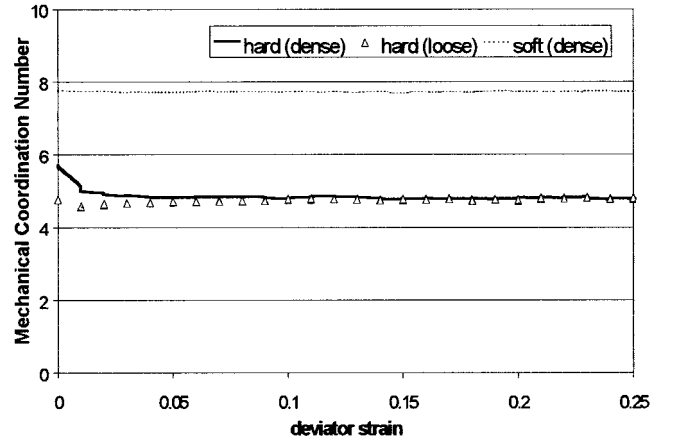


FIG. 9. Variation of the mechanical coordination number during shearing.

Antony [29] (with the same elastic properties as in the present soft system, but polydispersed), the deviator stress was fairly equal to the fabric deviator stress due to contacts with $f > 1$. Figure 12 shows the variation of the fabric deviator stress due to contacts with $f > 1$ during shearing. It is interesting to note that the following. (i) For both the dense and loose hard systems at steady (critical) state, the fabric deviator stresses contributed by the strong contacts have averaged out and attained a critical value. (ii) In the case of the soft system, although the maximum value of the normal contact force did attain a unique value on the force scale at the critical stage (Fig. 8), the fabric deviator stress contribution of the strong force chains could not attain this unique value at the critical state. It is worth remembering here that the probability distribution [Figs. 5 and 7(e)] of contacts for the soft system at isotropic and steady states is entirely half-Gaussian throughout the entire force scale that is used and seems to differ very little during shearing, except in a few instances. (iii) In Fig. 12, there occurs two local peaks, at one instance each for the dense and loose hard systems. One could not observe a direct correlation of this with the mechanical coordination number (i.e., the average number of load-bearing contacts), which in fact remains nearly the same (Fig. 9). However, Fig. 13 shows the typical variation of the total number of contacts for the hard dense system, bifurcated into two classes, i.e., contacts with (i) greater than average and (ii) less than average normal contact force. It is interesting to note that the fluctuations in Fig. 12 seem to tie in with the fluctuations shown in Fig. 13. The local drop in the number of strong contacts ($f > 1$), without a noticeable change in the coordination number of load-bearing contacts (Fig. 10), could suggest a local redistribution of strong forces.

IV. CONCLUDING REMARKS

To summarize, an attempt is made to search for a better understanding of the evolution of the contact normal force distribution during shearing using a nearly monodispersed system of particles in a three-dimensional periodic cell. The systems with different elastic properties (relatively hard and

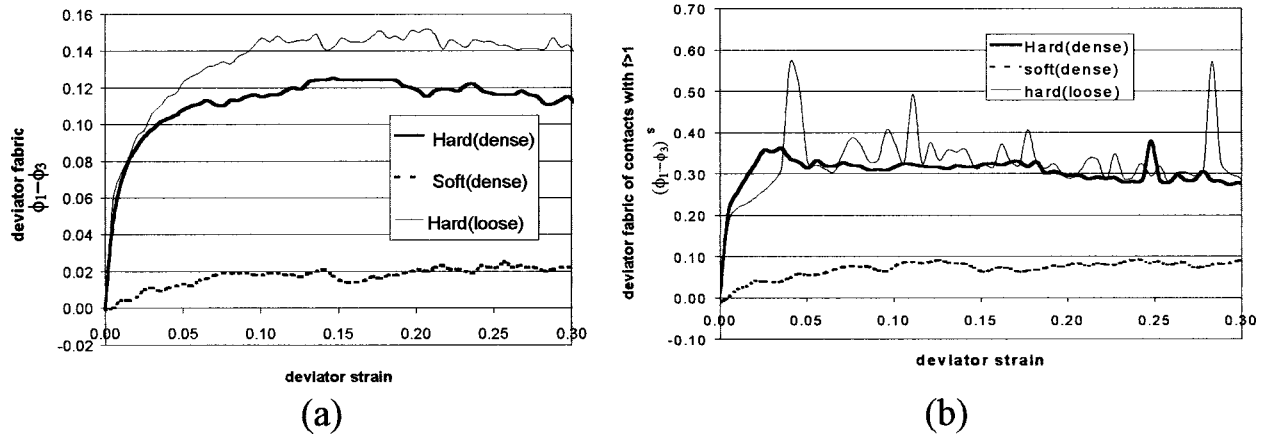


FIG. 10. Variation of the deviator fabric of hard and soft systems during shearing: (a) for the overall system; (b) for strong contacts only.

soft) and solid fraction (relatively dense and loose) were tested. It was observed that the contact normal stress contribution is the dominant contribution to the stress ratio q/p . Simulations have been carried out for both cases of noncohesive hard granular system and hard granular systems with low values of interface energy between the particles. The results seem to indicate that the amount of interface energy introduced between particles has not significantly changed the characteristic features of the force distribution compared with that of noncohesive particles sheared under the (high) constant mean stress condition, it nevertheless seems to improve the stability of the shear strength (q/p) curve. It would be interesting to investigate in future the effect of interface energy of the particles on the nature of the force distribution sheared at low mean stress levels or with particles having high values of interface energy, sheared under high mean stress levels. At low stress levels, the contribution of interface energy of particles could be more significant; this is yet to be confirmed. Also, the influence of interface energy on soft granular systems has yet to be investigated.

The distribution of contact normal force in a granular system during slow shearing, even for a noncohesive case, is sensitive to the shear history. The probability distribution for the contact normal force is quantified for the isotropic, peak, and steady states during shearing. It is interesting to note that the contact normal force distribution at peak shear strength for both cases of hard system (dense and loose) tends to decay exponentially throughout the force scale that is used. It is shown that, for the hard system, the probability distribution of the less than average contact normal force attains a different type of distribution during shearing, varying from a half-Gaussian distribution at the isotropic state through a uniform distribution, before being part of a completely exponential decay for the entire force scale at the peak state. For further shearing, the system follows a reverse cycle before eventually attaining a bimodal distribution at steady state, with forces less than average following a second-order polynomial distribution and forces greater than average following an exponential decay. It is worth mentioning here that an attempt was made to use a power-law distribution to fit the probability distribution of less than average contact normal forces (for example, see [21–23]). However, for the data

presented in this paper, the power-law distribution was satisfactory only for $\sim f < 0.5$ and hence is not presented here. For the case of hard (dense) and soft systems considered here, one could observe a well-defined peak in the distribution of weak forces, especially at isotropic and steady states. It should also be remembered that the peak in the weak force distribution changes during shearing and is clearly sensitive to the shear history. This is quite an important issue as previous researchers have reported different types of force distribution, especially for weak forces, for example a uniform distribution [7], power law [21–23], exponential [9,16,18] and Gaussian [10]. At this point in time, it is quite difficult to compare the present work with other researcher's experiments, as their results are not related to the shear history of the system (coupled with the solid fraction and elastic properties of the particles). However, the present simulations show that any of these distributions for weak forces is quite possible, depending largely on the shear history of the granular system. It has been shown that the force distribution also depends on the solid fraction and elastic properties of the particles. In both types of hard (dense and loose) system considered here, the probability distribution of the greater than average contact normal forces is an exponential decay for both the isotropic and steady states, and the exponent is not very different. The central message of this paper is that

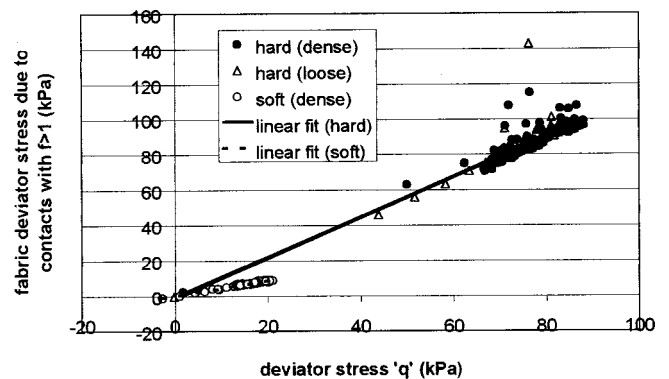


FIG. 11. Variation of the fabric deviator stress contributed by contacts with strong force with the deviator stress.

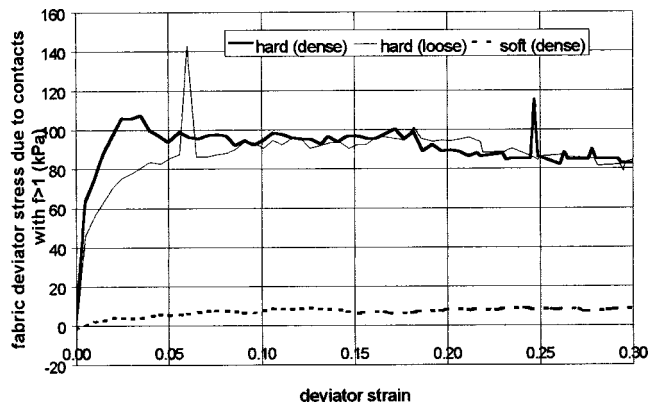


FIG. 12. Variation of the fabric deviator stress contributed by contacts carrying strong force during shearing.

force fluctuation in a granular medium is very sensitive to the shear history the system experiences. Hence a careful observation of the shear strain levels when carrying out experimental measurements and their interpretation is required.

It has been pointed out that the induced structural anisotropy developed during shearing is significantly dependent on the elastic modulus and solid fraction of the granular systems. For a granular system undergoing slow shearing, the shear strength of the system seems to depend on the ability of the system to build a strongly anisotropic fabric network of contacts carrying greater than average force. The present simulations were carried out with a relatively small number of particles due to the limitations in computer power available. However, further work from researchers in other laboratories is required to confirm the findings reported in this paper with simulations having a large number of particles,

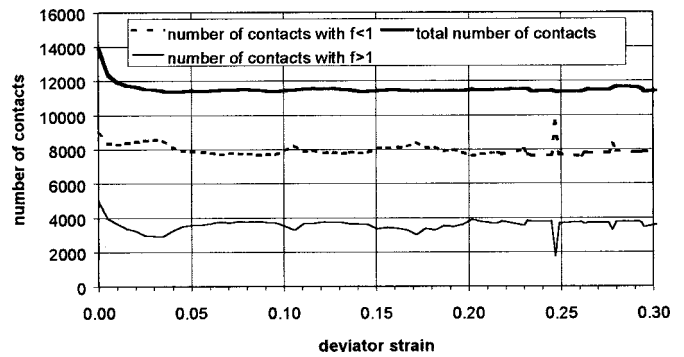


FIG. 13. Variation of the number of contacts during shearing.

thus allowing statistically more accurate calculations. It is worth mentioning here that an ongoing shear simulation for an entirely monodispersed particulate system (with properties identical to those reported here) has shown all the characteristics that are reported in this paper. Further investigation is in progress to determine the size effects of a submerged particle on the force and stress distribution [32]. This would give us an idea of the length scale in which the continuum theory would break down when studying the macroscopic behavior of granular media subjected to shearing.

ACKNOWLEDGMENTS

This work has been supported by ICI Technology Ltd., Wilton, UK and EPSRC, UK (Grant No. GR/M33907). The author is grateful to Dr. C. Thornton for useful conversations in the past. The author acknowledges the helpful comments from Professor M. Ghadiri, Dr. F. Radjai, Dr. C. Hodges, and J. Suberto.

-
- [1] R. Albert, M. A. Pfeifer, A.-L. Barabasi, and P. Schiffer, *Phys. Rev. Lett.* **82**, 205 (1999).
- [2] R. Behringer, H. Jaeger, and S. Nagel, *Chaos* **9**, 509 (1999).
- [3] M. E. Cates, J. P. Wittmer, J.-P. Bouchaud, and P. Claudin, *Chaos* **9**, 511 (1999).
- [4] S. F. Edwards and D. V. Grinev, *Chaos* **9**, 551 (1999).
- [5] P. G. Gennes, *Rev. Mod. Phys.* **71**, S374 (1999).
- [6] D. W. Howell, R. P. Behringer, and C. T. Veje, *Chaos* **9**, 559 (1999).
- [7] D. M. Mueth, H. M. Jaeger, and S. R. Nagel, *Phys. Rev. E* **57**, 3164 (1998).
- [8] F. Radjai, S. Roux, and J. J. Moreau, *Chaos* **9**, 544 (1999).
- [9] M. L. Nguyen and S. N. Coppersmith, *Phys. Rev. E* **59**, 5870 (1999).
- [10] M. G. Sexton, J. E. S. Socolar, and D. G. Schaeffer, *Phys. Rev. E* **60**, 1999 (1999).
- [11] C. Thornton and S. J. Antony, *Philos. Trans. R. Soc. London, Ser. A* **356**, 2763 (1998).
- [12] C. Thornton, *Geotechnique* **50**, 43 (2000).
- [13] A. V. Tkachenko and T. A. Witten, *Phys. Rev. E* **60**, 687 (1999).
- [14] A. Drescher and J. de Jong, *J. Mech. Phys. Solids* **20**, 337 (1972).
- [15] M. Oda and J. Konish, *Soils Found.* **14**, 25 (1974).
- [16] C. Liu, S. R. Nagel, D. A. Schecter, S. N. Coppersmith, S. Muajumdar, O. Narayan and T. A. Witten, *Science* **269**, 513 (1995).
- [17] D. W. Howell, R. P. Behringer, and C. T. Veje, *Chaos* **9**, 559 (1999).
- [18] S. N. Coppersmith, C. Liu, S. Majumdar, O. Narayan, and T. Witten, *Phys. Rev. E* **53**, 4673 (1996).
- [19] R. P. Behringer and B. Miller, *Powders and Grains '97*, edited by R. P. Behringer and J. T. Jenkins (Balkema, Rotterdam, 1997), pp. 333–336.
- [20] J. E. S. Socolar, *Phys. Rev. E* **57**, 3204 (1998).
- [21] F. Radjai, D. E. Wolf, S. Roux, M. Jean, and J. J. Moreau, *Powders and Grains '97* (Ref. [19]), pp. 211–214.
- [22] F. Radjai, M. Jean, J. J. Moreau, and S. Roux, *Phys. Rev. Lett.* **77**, 274 (1996).
- [23] F. Radjai, D. E. Wolf, M. Jean, and J. J. Moreau, *Phys. Rev. Lett.* **80**, 61 (1998).
- [24] F. Radjai and D. E. Wolf, *Granular Matter* **1**, 3 (1998).
- [25] L. E. Silbert, R. S. Farr, J. R. Melrose, and R. C. Ball, *J. Chem. Phys.* **111**, 4780 (1999).

- [26] P. A. Cundal and O. D. L. Strack, *Geotechnique* **29**, 47 (1979).
- [27] C. Thornton and K. K. Yin, *Powder Technol.* **65**, 153 (1991).
- [28] C. Thornton, *J. Appl. Mech.* **64**, 383 (1997).
- [29] C. Thornton and S. J. Antony, *Powder Technol.* **109**, 179 (2000).
- [30] M. Satake, in *Deformation and Failure of Granular Materials*, edited by P. A. Vermeer and H. J. Luger (Balkema, Rotterdam, 1982), pp. 63–68.
- [31] C. Thornton, in *Constitutive Modelling of Granular Materials*, edited by D. Kolymbas (Springer, New York, 2000), pp. 193–208.
- [32] S. J. Antony and M. Ghadiri (unpublished).